SPARTA: Spatially Attentive and Adversarially Robust Activation

Qing Guo, *Member, IEEE,* Felix Juefei-Xu, *Member, IEEE,* Changqing Zhou, Yang Liu, *Senior Member, IEEE,* Song Wang, *Senior Member, IEEE,*

Abstract—Adversarial training (AT) is one of the most effective ways for improving the robustness of deep convolution neural networks (CNNs). Just like common network training, the effectiveness of AT relies on the design of basic network components. In this paper, we conduct an in-depth study on the role of the basic ReLU activation component in AT for robust CNNs. We find that the spatially-shared and input-independent properties of ReLU activation make CNNs less robust to white-box adversarial attacks with either standard or adversarial training. To address this problem, we extend ReLU to a novel SPARTA activation function (Spatially attentive and Adversarially Robust Activation), which enables CNNs to achieve both higher robustness, *i.e.*, lower error rate on adversarial examples, and higher accuracy, *i.e.*, lower error rate on clean examples, than the existing state-of-the-art (SOTA) activation functions. We further study the relationship between SPARTA and the SOTA activation functions, providing more insights about the advantages of our method. With comprehensive experiments, we also find that the proposed method exhibits superior cross-CNN and cross-dataset transferability. For the former, the adversarially trained SPARTA function for one CNN (*e.g.*, ResNet-18) can be fixed and directly used to train another adversarially robust CNN (*e.g.*, ResNet-34). For the latter, the SPARTA function trained on one dataset (*e.g.*, CIFAR-10) can be employed to train adversarially robust CNNs on another dataset (*e.g.*, SVHN). In both cases, SPARTA leads to CNNs with higher robustness than the vanilla ReLU, verifying the flexibility and versatility of the proposed method.

1 INTRODUCTION

Ever since the identification of the adversarial examples [1] posing severe security threats to deep convolution neural networks (CNNs), studies have been pouring in to improve the adversarial robustness of the CNNs [2], [3], [4], [5], [6], [7], [8], [9], [10], [11], [12], [13]. Among these various methods, adversarial training [14], [15], [16] is regarded as one of the most effective attempts to improve the adversarial robustness of the neural network. Adversarial training aims at solving a min-max game by training on adversarial examples (on-the-fly) until the model learns to classify them correctly. Specifically, adversarial training is composed of two iterative steps, *i.e.*, an inner $\max$ step that finds the adversarial examples and an outer $\min$ step that carries out network parameters updates. Under this paradigm and in this work, we set out to investigate the impacts of basic network components, such as the commonly used ReLU activation, to the adversarial training effectiveness. Linear rectifier-based activation functions such as ReLU and variants enjoy the following advantages over the traditionally employed 'S'-shape activations such as Sigmoid and $\tanh$: ❶ less prone to vanishing gradient [17], ❷ more computationally efficient, and ❸ better convergence [18].

We argue that the spatially-shared and input-independent activating properties of the ReLU make CNNs under both standard training and adversarial training less robust to white-box adversarial attacks. Such uniformity across input spatial dimensions and different input data may be less ideal in suppressing adversarial patterns, rendering the adversarial training less effective, as we will thoroughly explore in experiments. To address such challenges, we design a novel activation function, *i.e.*, SPARTA: spatially-attentional activation for adversarial robustness, by allowing the activation to allocate different amounts of attention across input spatial dimensions, and to be dynamically adapted for each individual input. The flexibility in SPARTA, as opposed to the uniformity in ReLU, enables CNNs to achieve higher robustness (*i.e.*, lower error rate on adversarial examples) and accuracy (*i.e.*, lower error rate on clean examples) than CNNs based on the SOTA (non-spatially attentional and non-dynamic) activation functions.

We further investigate the relationships between our SPARTA and the SOTA search-based activation function, *i.e.*, Swish [21], and feature denoising method [20], providing insights about the advantages of our method. Moreover, comprehensive evaluation demonstrates two important properties of our method: 1) *superior transferability across CNNs*. The adversarially trained activation function for one CNN (*e.g.*, ResNet-18) can be fixed to train another adversarially robust CNN (*e.g.*, ResNet-34), achieving higher robustness than the one using ReLU; 2) *superior transferability across datasets*. The SPARTA function trained on one dataset (*e.g.*, CIFAR-10) can be employed to train adversarially robust CNNs on another dataset (*e.g.*, SVHN) and helps achieve higher robustness than CNNs with ReLU. These properties demonstrate the advantage of SPARTA in terms of flexibility and versatility.

2 RELATED WORK

Adversarial training methods. Adversarial training generates adversarial examples on-the-fly for training CNNs [14], [15], [16], [22]. Athalye *et al*. [23] demonstrates that projected gradient descent (PGD)-based adversarial training can be considered as the current state-of-the-art defense method. Tramèr *et al*. [24] proposes to perform adversarial training with the adversarial examples generated from several pre-trained models. Then, a series of works are proposed to further enhance the PGD-based adversarial training via [20],

• *Q. Guo, C. Zhou, and Y. Liu are with Nanyang Technological University, Singapore. F. Juefei-Xu is with Alibaba Group, Sunnyvale, CA 94085, USA. S. Wang is with Department of Computer Science and Engineering, University of South Carolina, Columbia, SC 29208, USA.*

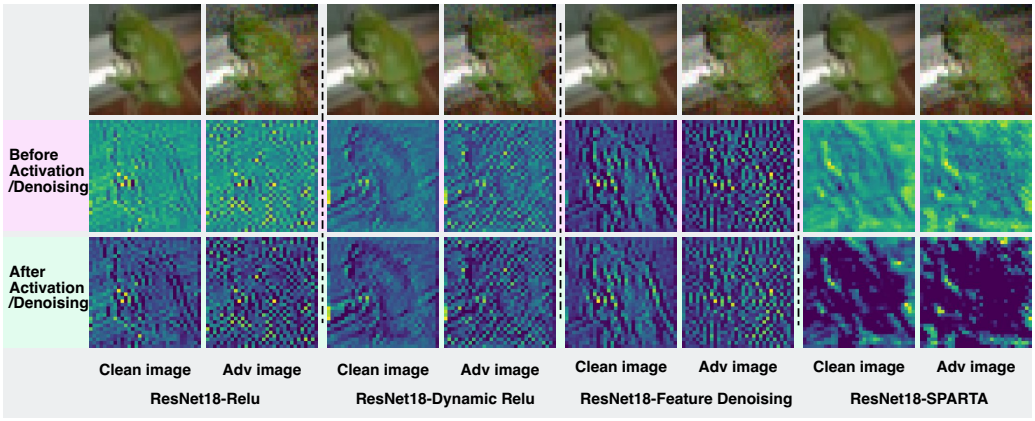

Fig. 1: Visualization results of feature maps before and after activation for ReLU, Dynamic ReLU [19], and SPARTA or feature denoising for [20]. Note that, all CNNs are based on the ResNet-18 backbone under standard training and the feature maps are from the last layer of the first group.

[25], [26], [27], [28], [29]. In particular, Goodman *et al*. [29] notes the importance of image-level attention for adversarial training while our work focuses on feature-level attention realized by the newly designed activation function. Nevertheless, limited works so far have studied the effects of basic network components such as the ReLU activation to adversarial training. In this work, we discuss the limitations of ReLU for adversarial training (*i.e.*, the spatially-share and input-independent properties) and further propose the spatially-attentional activation function for more higher adversarial robustness.

Other Adversarial robustness enhancement methods. Besides adversarial training, numerous studies have shown to be effective towards enhancing adversarial robustness of CNNs: (1) The ones that involve non-differentiable operators, intentionally or unintentionally. The introduced non-differentiability and numeric instability lead to incorrect and degenerate gradients such as applying the thermometer encoding [3], performing various image transformations (cropping, bit-depth reduction, *etc*.) [9], and using local intrinsic dimensionality to characterize adversarial subspaces [30]. However, they may be circumvented by computing the backward pass using a differentiable approximation of the function [23]. (2) The ones involve either a randomized network such as [5], [6], [7] or randomly transformed inputs such as [4], [8], [9], which hinder the correct estimation of the true gradient when using a single sample of the randomness. However, they may be countered by computing the gradient correctly over the expected transformation to the input [23]. (3) The ones involve input data purification such as high-level representation guided denoiser [13], pixel deflection [10], PixelDefend [11], and Defense-GAN [12]. However, re-parameterization can greatly diminish these attempts for improving the adversarial robustness of the CNNs [23]. (4) Others such as defensive distillation [2] and adversarially robust architecture [31].

Activation functions. In recent years, quite a few works attempt to study how to improve the ReLU activation function from the viewpoint of enhancing CNNs' accuracy [19], [21], [32], [33], [34], [35], [36], [37], [38]. However, few of them investigate from the viewpoint of the adversarial training. In Sec. 3, we summarize eight existing representative activation functions and discuss their properties from spatial-wise, dynamic, and attentional properties via Table 1.

TABLE 1: Main activation functions for accuracy enhancements and adversarial robustness.

Designing for	Activation	Spatial-wise	Dynamic	Attentional
Accuracy Enhancement	ReLU	✗	✗	✗
	LeakyReLU	✗	✗	✗
	PReLU	✗	✗	✗
	ELU	✗	✗	✗
	GELU	✗	✗	✗
	Swish	✗	✗	✗
	Dynamic ReLU	✓	✓	✗
Adversarial Robustness	Smooth ReLU	✗	✗	✗
	SPARTA (Ours)	✓	✓	✓

3 Existing ReLU Activations and Challenges

Given an input tensor $\mathbf{X}$, the widely used activation function, *e.g.*, ReLU, can be represented as

$$\mathbf{Y}_p = \max(\mathbf{X}_p, 0), \ \forall p \in \mathcal{P}, \tag{1}$$

where $\mathbf{X}_p$ is the p-th element in $\mathbf{X}$ and $\mathcal{P}$ denotes the set of all element positions of $\mathbf{X}$. The corresponding derivative of this function w.r.t. the input $\mathbf{X}$ is

$$\frac{d\mathbf{Y}_p}{d\mathbf{X}_p} = \begin{cases} 1, & \text{if } \mathbf{X}_p \geq 0, \\ 0, & \text{if } \mathbf{X}_p < 0, \end{cases} \quad \forall p \in \mathcal{P}. \tag{2}$$

We argue that *such unified activation across all elements of input tensor during the both forward and backward processes makes the adversarial training less effective.* Intuitively, the white-box adversarial attack can be easily achieved due to: ❶ for the forward process, both clean and corrupted elements in $\mathbf{X}$ are equally activated, making the adversarial noise easily propagate to the deeper layers, thus affecting the prediction results, directly. ❷ during the back-propagation of the white-box attack, the gradients of all elements in $\mathbf{X}$ pass evenly the activation function for generating the adversarial perturbations, making the white-box attack researching optimized solution easily. We will validate these in Sec. 4.2.

To overcome the above limitations, we take the following two factors into consideration to design the novel activation function: ❶ a spatial-wise and attentional activation should be developed, which makes different elements in $\mathbf{X}$ have different activation conditions and semantic-related elements be preserved while perturbations being suppressed. For example, the elements corrupted by adversarial noise should be suppressed during the activating while the clean

ones should be preserved. ❷ The activation should be dynamic, that is, it could be tuned to adapt to different inputs. Actually, the first factor indicates that the activation should have the spatial-wise and attentional properties, where the semantic and clean elements should be highlighted while the corrupted ones should be suppressed. The second factor indicates that the activated value of each element should consider the whole input.

Although some recent attempts have been made to explore how to improve the ReLU [32] from the angle of accuracy enhancement, including LeakyReLU [33], PReLU [35], ELU [36], GELU [39], Swish [21], Dynamic ReLU [19], and Smooth ReLU [38], none of them could perfectly fit the above two key factors. We summarize their basic information in terms of the spatial-wise, attentional and dynamic properties in Table 1. Among these improved ReLU variants, LeakyReLU and exponential linear unit (ELU) extend the activation range to negative values while all input elements share the same activation condition, which cannot be tuned according to inputs. PReLU adds extra learnable parameters to the basic ReLU, which are trainable but fixed for different inputs after training. Dynamic ReLU is a spatial-wise and dynamic activation function where each input element has an exclusive activation function represented by several linear functions whose slope and bias parameters are dynamically predicted by a network. Nevertheless, dynamic ReLU is specifically designed for accuracy enhancement, which lacks generality and does not consider the attentional requirement of adversarial robustness, failing to suppress adversarial corrupted elements. As shown in Fig. 1, the feature maps of ResNet-18 with dynamic ReLU before and after activation are almost the same and the noise patterns are not removed. We further discuss the quantitative results in Sec. 5.2. In addition to above activations, MaxOut [34] and squeeze-and-excitation networks (SE) [37] can be also used to realize activations as introduced in [19]. MaxOut has learnable parameters for the ReLU and can be offline trained but the parameters cannot change according to different inputs. SE lets the activation rely on the input and realizes dynamic activation that however is shared by all elements.

4 Methodology

4.1 Spatially Attentional Activation Function

Formulation. To address the robustness challenges, we propose the SPARTA. Given an input tensor $\mathbf{X}$, we have

$$\mathbf{Y}_p = \max(\mathbf{X}_p, 0) \cdot \phi_\theta(\mathbf{X})[p], \ \forall p \in \mathcal{P}, \tag{3}$$

where $\phi_\theta(\cdot)$ is a sub-network with θ as the parameters. The sub-network takes all elements of $\mathbf{X}$ as inputs, predicts a new tensor that has the same size with $\mathbf{X}$, and assigns a weight for each element of $\mathbf{X}$. Hence, $\phi_\theta(\mathbf{X})[p]$ denotes the p-th element of $\phi_\theta(\mathbf{X})$ and we have $\{0 \leq \phi_\theta(\mathbf{X})[p] \leq 1 | \forall p, p \in \mathcal{P}\}$. Then, we get the derivative of Eq. (3) w.r.t. the input $\mathbf{X}$

$$\frac{d\mathbf{Y}_p}{d\mathbf{X}_p} = \begin{cases} \phi_\theta(\mathbf{X})[p] + \mathbf{X}_p \frac{\partial \phi_\theta(\mathbf{X})}{\partial \mathbf{X}_p}, & \text{if } \mathbf{X}_p \geq 0, \\ 0, & \text{if } \mathbf{X}_p < 0, \end{cases} \quad \forall p \in \mathcal{P}. \tag{4}$$

Comparing with the formulations in Eq. (1) and (2), we notice that: ❶ for the forward process, each activated element is further processed by a scalar estimated from $\phi_\theta(\mathbf{X})$ that considers the whole input. Intuitively, the pre-trained $\phi_\theta(\cdot)$ decides whether the p-th element of $\mathbf{X}$ should be suppressed according to the understanding of the whole input. ❷ In terms of the backward process, in contrast to Eq. (2), the activated elements' gradients are not propagated to the earlier layers directly but determined by $\phi_\theta(\mathbf{X})$ and $\mathbf{X}_p \frac{\partial \phi_\theta(\mathbf{X})}{\partial \mathbf{X}_p}$. When $\phi_\theta(\cdot)$ is a deep neural network with the Sigmoid function as the last layer for activation, the gradient of its input $\frac{\partial \phi_\theta(\mathbf{X})}{\partial \mathbf{X}_p}$ tends to be very small [40]. Then, we can say that $\frac{d\mathbf{Y}_p}{d\mathbf{X}_p}$ mainly relies on $\phi_\theta(\mathbf{X})[p]$, meaning that the white-box attack based on back-propagation is affected by the $\phi_\theta(\mathbf{X})[p]$. For example, if $\mathbf{X}_p$ is the element that should be adversarially corrupted for effective attack and we have $\phi_\theta(\mathbf{X})[p] < 1$, the white-box attack would be harder to be optimized due to the less effective back-propagated gradients. We will validate the two concerns under both standard training and adversarial training in Sec. 4.2. Note that, Eq. (4) does not harm the CNN's accuracy under standard training and can even be helpful to achieve lower error rate. As shown in Table 2, ResNet-18s with our activation function (*i.e.*, SPARTA-w/o-DPNet and SPARTA that will be introduced in Sec. 4.1) achieve lower top-1 error rate than the network using ReLU under both standard and adversarial training.

Architecture of $\phi_\theta(\cdot)$. A simple architecture for $\phi_\theta(\cdot)$ can be the CNN that takes the $\mathbf{X}$ as the input and outputs a tensor having the same size to decide the activation weights of

TABLE 2: Comparing ResNet-18s equipped with ReLU, SPARTA-w/o-DPNet, and SPARTA, respectively.

	ResNet-18	Top-1 error on Adv. Images PGD-10	PGD-30	PGD-50	Top-1 err. on Clean Img
Adv. Train. on PGD-10	ReLU	31.54%	68.93%	75.64%	15.66%
	SPARTA -w/o-DPNet	29.43%	66.13%	72.35%	15.44%
	SPARTA	29.31%	65.81%	72.55%	15.48%
Std. Train.	ReLU	100.0%	100.0%	100.0%	7.71%
	SPARTA -w/o-DPNet	99.94%	100.0%	100.0%	6.98%
	SPARTA	99.85%	100.0%	100.0%	6.90%

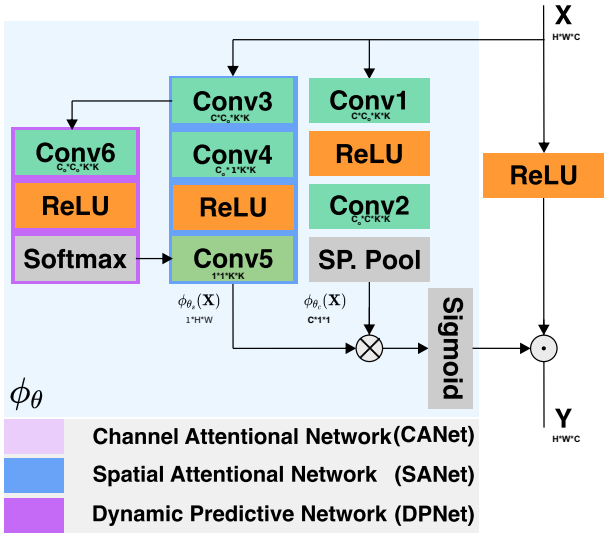

Fig. 2: Proposed *dynamic spatial-channel-attentional network* ($\phi_\theta(\cdot)$) containing 3 sub-networks, *i.e.*, channel attentional net ($\phi_{\theta_c}(\cdot)$), spatial attentional net ($\phi_{\theta_s}(\cdot)$), and dynamic predictive net ($\phi_{\theta_d}(\cdot)$), where $\theta = \{\theta_s, \theta_c, \theta_d\}$. The Sp. Pool performs spatial pooling and generate channel attentional vector.

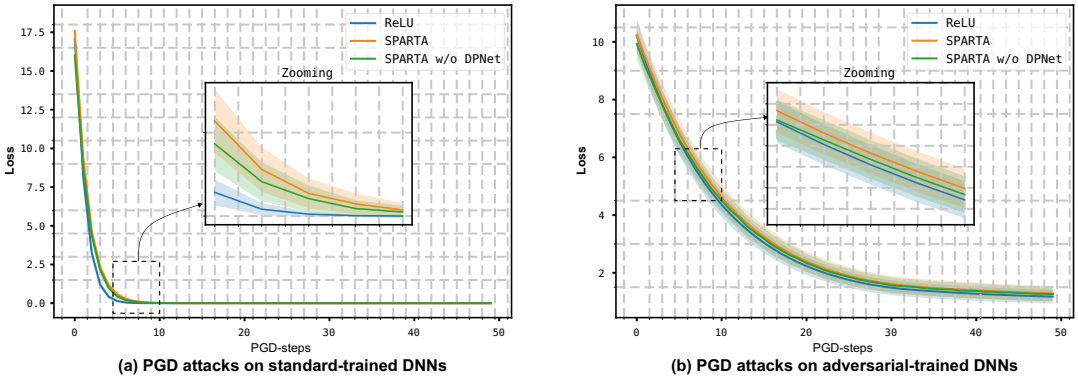

Fig. 3: Comparing loss values of ResNet-18 with ReLU, SPARTA, and SPARTA-w/o-DPNet during the PGD attack under standard training (a) and adversarial training (b).

each element. However, such an architecture requires a large number of parameters, making the whole network difficult to train. Moreover, since an activation can be deployed at different locations of a CNN (*i.e.*, from the shallow layers to deep ones), the inputs $\mathbf{X}$ would be diverse (*e.g.*, the $\mathbf{X}$ from shallow layers mainly contain spatial details while the deep ones focus on semantic information). Hence, a dynamic architecture that tunes the attentional network according to the input is highly desired. To this end, we propose the *dynamic spatial-channel-attentional network (DSCANet)* as $\phi_\theta(\cdot)$

$$\phi_\theta(\mathbf{X}) = \text{Sigmoid}(\phi_{\theta_s}(\mathbf{X}) \otimes \phi_{\theta_c}(\mathbf{X})), \tag{5}$$

where '$\otimes$' is the outer production, and $\phi_{\theta_s}(\cdot)$ and $\phi_{\theta_c}(\cdot)$ denote the spatial-attentional network (SANet) and channel-attentional network (CANet), respectively. When we have $\mathbf{X} \in \mathbb{R}^{H\times W\times C}$, $\phi_{\theta_s}(\mathbf{X}) \in \mathbb{R}^{H\times W}$ is the spatial attentional map across all channels and $\phi_{\theta_c}(\mathbf{X}) \in \mathbb{R}^{1\times 1\times C}$ is the channel attentional vector across all spatial positions. Moreover, inspired by the dynamic convolution [41], we construct a dynamic predictive network (DPNet) to predict the parameters of the last layer of SANet according to the input. As a result, we realize the desired dynamic property of activation. As shown in Fig. 2, the whole architecture contains three sub-networks where the sizes of convolution layers and tensors are shown at the bottom, and Conv5's parameters are estimated from DPNet. The parameter number of the DSCANet is determined by the channel number of $\mathbf{X}$ (*i.e.*, C) and the kernel size of convolution layers for the three sub-networks (*i.e.*, K shown in the Fig. 2). To avoid heavy cost, we set $K = 1$ and the channel-related parameter, *i.e.*, $C_o = \min(256, C)$. We compare cost on parameters with other activations in the experiment section. We will further discuss the influence of different architectures in the Sec. 4.2.

4.2 Analysis of SPARTA

We aim to analyze SPARTA by comparing with the basic ReLU in Sec. 3, and answer the following questions: Does the SPARTA help achieve higher adversarial robustness under *standard training* and *adversarial training*, respectively? Do the advantages stem from the spatial-wise, dynamic, and attentional architectures? Moreover, we discuss how to perform replacement with SPARTA in a CNN.

4.2.1 Setup

For a comprehensive analysis of the proposed activation function, we use ResNet-18 [42] as the backbone network and modify it by replacing the last ReLU layers of the four groups in ResNet-18 with our SPARTA, respectively. We further discuss the influence of replacement strategies in Sec 4.2.4. Then, we conduct the image classification task on CIFAR-10 dataset, comparing the top-1 error rate of the raw ResNet18 and the modified one under both standard training and adversarial training. For adversarial training, we follow the setups in [20] and perform the targeted projected gradient descent (PGD) attack [43] to generate adversarial examples with the step size of 1.0, and the maximum perturbation of 16.0. The targeted class is selected uniformly at random. The same setup is also used in the testing. We implement three PGD attacks according to the iteration number of 10, 30, and 50 and denote them as PGD-10, PGD-30, and PGD-50, respectively. Note that, in all sub-sequence experiments, the top-1 error rate on adversarial (adv.) images means that we first generate adversarial examples by using PGD to attack the evaluated CNN and calculate the classification error rate on these adversarial images. The sub-network and CNN are jointly trained, where we set the learning rate to be 0.1 with the $10\times$ attenuation at the 30th and 60th epochs, and the weight decay is set to be 1e$-$4. In Sec. 5.3, we also show that pre-trained SPARTA on one model and dataset can be fixed and benefit adversarial training of another model.

4.2.2 Dynamic and attentional activation benefits adversarial robustness

Table 2 summarizes the top-1 error rates of three versions of ResNet-18 on the adversarial and clean images of CIFAR-10 under both adversarial and standard training, from which we have the following observations and conclusions: ❶ Compared with ReLU, SPARTA does let the CNN achieve much better adversarial robustness (*i.e.*, lower top-1 error rate on adversarial examples from white-box PGD attacks, *e.g.*, 75.64% vs. 72.55% on PGD-50) under adversarial training while further improving the accuracy on clean images (*e.g.*, 15.66% vs. 15.48%), concluding that SPARTA *improves adversarial robustness without the sacrifice of classification accuracy for clean images*. ❷ In terms of the standard training, SPARTA leads to lower top-1 error rate (*i.e.*, 100% for ReLU vs. 99.85% for SPARTA) under the PGD-10 while achieving much higher accuracy (*i.e.*, lower error rate on clean images), demonstrating that SPARTA *does not rely on adversarial training and still benefits to both adversarial robustness and accuracy under standard training*. ❸ Compared with SPARTA-w/o-DPNet where the DPNet in $\phi_\theta(\cdot)$ is removed, SPARTA

TABLE 3: Comparing ResNet-18s equipped with SPARTA according to different spatial-wise setups defined by Eq. (6), respectively. The best results are highlighted.

ResNet-18 with SPARTA	Top-1 error on Adv. Images PGD-10	PGD-30	PGD-50	Top-1 err on Clean Img
$N = 1$	**29.73%**	**65.93%**	**72.98%**	15.25%
$N = 2$	30.11%	66.27%	73.40%	14.98%
$N = 4$	30.17%	66.58%	73.45%	15.07%

TABLE 4: Comparing ResNet-18s with SPARTA employed at different depths. The best and second results are highlighted.

ResNet-18: replacing ReLU with SPARTA at	Top-1 error on Adv. Images PGD-10	PGD-30	PGD-50	Top-1 err on Clean Img
$G_1.B_2$	32.33%	67.23%	74.38%	17.41%
$G_2.B_2$	31.61%	67.76%	75.50%	15.68%
$G_3.B_2$	31.15%	68.12%	75.01%	15.77%
$G_4.B_2$	**29.73%**	**65.93%**	**72.98%**	15.25%
$G_{\{1,2,3,4\}}.B_{\{1,2\}}$	31.32%	65.83%	**72.28%**	16.70%
$G_{\{1,2,3,4\}}.B_2$	**29.31%**	**65.81%**	72.55%	15.48%

achieves lower top-1 errors under all PGD attacks in the cases of adversarial and standard training, confirming that *the dynamic activation function via the proposed DPNet helps the CNN achieve higher adversarial robustness.* ❹ When further comparing ReLU with SPARTA-w/o-DPNet, we see that ResNet-18 with SPARTA-w/o-DPNet has lower top-1 error rates on most of the PGD attacks and clean images. Under the standard training, SPARTA-w/o-DPNet always improves the CNN with lower error rates on clean images. These results demonstrate *attentional activation introduced by the spatial attentional network and channel attentional network does enhance the CNNs' adversarial robustness and accuracy and also benefits the standard training for higher accuracy*.

To better understand the above results, we conduct an experiment to compare the loss values of pre-trained CNNs during PGD attacks, to validate if SPARTA makes the adversarial attack harder as explained in Sec. 4.1. Specifically, we perform PGD-50 on 20% examples of CIFAR-10 testing dataset and collect the loss values during the optimization process. Then, we calculate the mean and standard deviation of loss values at each iteration step across all examples, and draw three plots of the ResNet-18s with ReLU, SPARTA-w/o-DPNet, and SPARTA, respectively. As shown in Fig. 3, we see that the loss values of CNNs based on SPARTA and SPARTA-w/o-DPNet are always larger than that of ReLU-based CNNs along the iteration. It demonstrates that *the proposed attentional and dynamic activation function does make the optimization of adversarial attack harder for both adversarial and standard trained CNNs.*

4.2.3 Spatial-wise activation benefits adversarial robustness

In addition to the attentional and dynamic properties, we further analyze the importance of spatial-wise activation. To this end, we set spatial-neighboring elements of $\mathbf{X}$ sharing the same attentional scores and control the neighboring size to study the influence of spatial-wise activation. We reformulate Eq. (3) to represent the above process as

$$\mathbf{Y}_p = \max(\mathbf{X}_p, 0) \cdot \phi_\theta(\mathbf{X})[\lfloor \frac{p}{N} \rfloor], \ \forall p \in \mathcal{P}, \tag{6}$$

where we set the output size of $\phi_\theta(\mathbf{X})$ to be $\frac{H}{N} \times \frac{W}{N} \times C$ and N controls the neighboring size. For example, when we set $N = 2$, every four elements in $\mathbf{X}$ share the same attentional scores; when we have $N = 1$, Eq. (6) becomes Eq. (3), *i.e.*, each element has its exclusive attentional score.

To analyze the effects of different N, we modify ResNet-18 by replacing the fourth block's ReLU with SPARTA and obtain three CNNs by setting $N = 1, 2, 4$. Then, we perform the adversarial training and evaluate the robustness and accuracy, respectively. We present the results in Table 3 with the following observations: ❶ for all three PGD attacks, the top-1 error rate on adversarial images increases as the N becomes larger (*i.e.*, more elements share the same attentional score), indicating that *spatial-wise activation benefits the adversarial robustness.* ❷ In terms of the results on clean images, the CNN with $N = 1$ has higher top-1 error rate than the ones with $N = 2$ and $N = 4$, which indicates the spatial-wise activation could reduce the accuracy to some extent. Even though, SPARTA with $N = 1$ still enables the CNN to achieve lower error rate than ReLU.

4.2.4 Effects of SPARTA's Locations in CNNs

Since SPARTA contains extra parameters for the three sub-networks in Fig. 2, it is ideal to perform as fewer ReLU replacements as possible to avoid heavy costs. To this end, we study the influence of replacement positions based on the widely used ResNet and take the representative ResNet-18 as a representative case to study. ResNet-18 contains four groups and each group has two blocks. We focus on replacing the last ReLU layer of each block and set the following strategies: *First*, we replace the last ReLU layer of the second block of each group with our SPARTA and obtain four CNNs denoted as ResNet-18-$G_i.B_2$ where i denotes the ith group of ResNet-18 and B_2 represents the second block. This setup helps explore the influence of SPARTA at different depths of a CNN. *Second*, we perform the replacements on all groups simultaneously and study whether more substitutions lead to better adversarial robustness. In particular, we consider two versions denoted as 1) $G_{\{1,2,3,4\}}.B_{\{1,2\}}$ and 2) $G_{\{1,2,3,4\}}.B_2$, respectively. The first one replaces the last ReLU layers of the two blocks of all groups, while the second one only conducts replacement on the second block of all groups.

4.3 Relationship to existing methods and beyond

Relationship to Swish and beyond. More recently, [38] identifies the importance of the smooth activation function for adversarial training and shows the search-based activation function, *i.e.*, Swish [21], which achieves the state-of-the-art adversarial robustness and can be represented as

$$\mathbf{Y}_p = \mathbf{X}_p \cdot \text{Sigmoid}(\mathbf{X}_p), \ \forall p \in \mathcal{P}. \tag{7}$$

Meanwhile, we can reformulate the SPARTA by combining Eq. (3) and (5) and have

$$\mathbf{Y}_p = \max(\mathbf{X}_p, 0) \cdot \text{Sigmoid}((\phi_\theta(\mathbf{X}))[p]), \tag{8}$$

$$\phi_\theta(\mathbf{X})[p] = (\phi_{\theta_s}(\mathbf{X}) \otimes \phi_{\theta_c}(\mathbf{X}))[p], \ \forall p \in \mathcal{P}. \tag{9}$$

Comparing Eq. (7) with Eq. (8), we can see that Swish is very similar to our SPARTA, but having two major differences: ❶ the first term $\mathbf{X}_p$ in the right part of Eq. (7) is further

TABLE 5: Comparing ResNet-18s with Swish, Swish-ReLU, and SPARTA under 3 PGD attacks. The best results are highlighted.

ResNet-18 with	Top-1 error on Adv. Images PGD-10	PGD-30	PGD-50
Swish	30.38%	68.65 %	76.21%
Swish-ReLU	30.10%	67.70%	75.07%
SPARTA	**29.31%**	**65.81%**	**72.55%**

processed via ReLU in Eq. (8). ❷ In terms of the variable in Sigmoid$(\cdot)$, Eq. (7) uses $\mathbf{X}_s$ itself while Eq. (8) adopts the spatial and channel attentions that consider all elements in $\mathbf{X}$. We have demonstrated the advantages of the spatial and channel attentions in Sec. 4.2.2. Here, we further study the influence of the first difference and show that the *adversarial robustness of Swish can be further enhanced by simply adding the ReLU to Eq. (7)*. As shown in Table 5, when equipping Swish with ReLU (*i.e.*, Swish-ReLU), the top-1 error rates on all PGD attacks decrease.

Relationship to feature denoiser. Xie *et al.* [20] improves the adversarial robustness of CNNs by adding extra blocks for feature denoising, inspired by the fact that the pixel-level adversarial noise poses large perturbations to the deep features and leads to noisy activation overwhelming the true ones, resulting in erroneous predictions. SPARTA can also be regarded as a denoising block and has the capability of feature denoising, since the perturbed elements in $\mathbf{X}$ are selectively activated or suppressed according to the predictive results of $\phi_\theta(\mathbf{X})$. As shown in Fig. 1, in terms of ResNet-18-SPARTA, we see obvious noise patterns before the activation, which are suppressed after the activation. As a result, the feature map after activation becomes similar to the clean one. Compared with the method of [20], SPARTA has the following difference and advantages: ❶ from the viewpoint of denoising, SPARTA uses multiplication for denoising and dynamically tunes the parameters via DPNet according to the inputs while the feature denoising method adopts the addition with fixed denoising operations. The higher level of flexibility of SPARTA helps CNNs achieve much better adversarial robustness. Please find the quantitative analysis in Sec. 5.2. ❷ SPARTA is a new activation function that can directly replace existing ReLUs in a CNN without changing its original architecture. On the other hand, the feature denoising method needs to add new blocks to existing CNNs, requiring extra adaption costs.

5 EXPERIMENTS

5.1 Setup

Following the setup in Sec. 4.2.1, we further consider ResNet-18 and ResNet-34 [42] as the backbones and evaluate on CIFAR-10 [44], Tiny-ImageNet, and SVHN datasets [45], mainly investigating two questions: How is the performance of SPARTA compared with state-of-the-art activation functions, including ReLU [32], ELU [36], GELU [39], Swish [21], [38], Dynamic ReLU (DyReLU) [19], and the feature denoising method (FD) [20]? Can SPARTA be shared across CNNs, and can SPARTA be shared across datasets?

5.2 Comparison with state-of-the-art activations

We compare our SPARTA with 5 SOTA activations and the feature denoising method through ResNet-18 and ResNet-34 architectures. Note that, we implement all baseline activations according to their public released codes. As the results on CIFAR-10 shown in Table 6, we have the following observations: ❶ Under adversarial training, CNNs with SPARTA achieve the lowest top-1 error on all three levels of PGD attack as well as lower top-1 error than CNNs with ReLU, demonstrating that *the proposed activation does help CNNs realize better adversarial robustness without sacrificing the accuracy.* ❷ Under standard training, CNNs with SPARTA have the second best accuracy (*i.e.*, second lowest top-1 error on clean images), indicating that *the proposed activation architecture not only benefits to adversarial training for better robustness but also helps achieve higher accuracy.* Then, we further conduct the comparison on SVHN and Tiny-ImageNet datasets and present the results in Table 7. Similar with the results on CIFAR-10, our SPARTA has lower top-1 errors than all other baseline methods under PGD-10, 30, and 50 attacks with similar accuracy with ReLU on the clean images, which further demonstrates the advantages of our method against adversarial attacks.

In addition to the error rate comparison, we further compare SPARTA and six baseline methods about their model size in Table 6. Compared with baseline methods, we see that SPARTA-v2 with similar model size achieves lower error rate under PGD-30 and PGD-50.

5.3 Transferability across CNNs

We study the transferability of SPARTA across CNNs, *i.e.*, we regard the pre-trained SPARTA borrowed from one CNN as the activation function for another CNN and see if it achieves better adversarial robustness. We take ResNet-18 and ResNet-34 as the backbones and conduct the following steps based on CIFAR-10 dataset: *First*, we adversarially train a CNN (*e.g.*, ResNet-34) equipped with SPARTA and obtain the pre-trained SPARTA at different blocks. We denote the pre-trained activations as $\text{SPARTA}_{\text{Res34}}$. *Second*, we equip another CNN (*e.g.*, ResNet-18) with $\text{SPARTA}_{\text{Res34}}$ and perform the adversarial training without updating the parameters of $\text{SPARTA}_{\text{Res34}}$. Similarly, we can also train ResNet-34 by using the pre-trained SPARTA from ResNet-18 (*i.e.*, $\text{SPARTA}_{\text{Res18}}$). As shown in Table 8, we see that: ❶ CNNs (*i.e.*, ResNet-18 and ResNet-34) with the transferred SPARTA achieve lower top-1 error rate than CNNs using ReLU under all three attacks (*i.e.*, PGD-10, 30, 50) and the clean images. Such results demonstrate that *pre-trained* SPARTA *has the transferability to some extent and can help other CNNs achieve better adversarial robustness and accuracy than the ones using ReLU.* ❷ Compared with the CNNs with standard SPARTA (*e.g.*, ResNet-34 with $\text{SPARTA}_{\text{Res34}}$) whose parameters are jointly updated during adversarial training, the CNNs with transferred SPARTA (*e.g.*, ResNet-34 with $\text{SPARTA}_{\text{Res18}}$) get worse adversarial robustness (*i.e.*, higher error rate under the three attacks). For example, ResNet-34 with $\text{SPARTA}_{\text{Res34}}$ obtains much lower top-1 error rates than ResNet-34 with $\text{SPARTA}_{\text{Res18}}$ under all 3 PGD attacks and also has slightly lower error on clean images, *i.e.*, 14.47% vs. 14.60%.

5.4 Transferability across Datasets

We further study the transferability of SPARTA across datasets. Specifically, we adversarially train a ResNet-

TABLE 6: Comparing SPARTA with ReLU, ELU, GELU, feature denoising operation (FD), Dynamic ReLU (DyReLU), and Smooth ReLU (SmReLU) by equipping them to ResNet-18 and ResNet-34 for adversarial training and standard training on CIFAR-10 dataset. The best and second results are highlighted.

	ResNet-18						ResNet-34					
	Adv. Training Error on Adv. Imgs			Error on Clean Imgs	Std. Training Error on Clean Imgs	Size	Adv. Training Error on Adv. Imgs			Error on Clean Imgs	Std. Training Error on Clean Imgs	Size
	PGD-10	PGD-30	PGD-50				PGD-10	PGD-30	PGD-50			
ReLU	31.54%	68.93%	75.64%	15.66%	7.71%	11.17 M	31.00%	67.88%	75.15%	17.18 %	7.36%	21.28 M
ELU	31.44%	67.57%	72.98%	17.08%	7.99%	11.17 M	31.31%	67.67%	74.02%	17.16%	7.88%	21.28 M
GELU	**30.27%**	68.95%	75.30%	14.55%	6.85%	11.17 M	**29.66%**	65.95%	**73.68%**	**15.03%**	6.52%	21.28 M
FD	31.81%	**67.03%**	**73.52%**	16.81%	7.99%	11.87 M	30.71 %	**65.72%**	73.90 %	17.49%	8.05%	21.98 M
DyReLU	32.57%	68.54%	75.08%	16.97%	7.40%	11.79 M	31.56%	68.40%	75.84%	17.63%	8.78%	21.90 M
SmReLU	30.38%	68.65%	76.21%	14.26%	7.00%	11.17 M	32.20%	67.51%	74.42%	16.74%	7.28%	21.28 M
SPARTA	**29.31%**	**65.81%**	**72.55%**	15.48%	6.90%	11.99 M	**29.17%**	**64.13%**	**72.91%**	**14.47%**	6.78%	22.11 M

TABLE 7: Comparing with ReLU, ELU, GELU, feature denoising operation (FD), Dynamic ReLU (DyReLU), and Smooth ReLU (SmReLU) by equipping them to ResNet-18 for adversarial training on Tiny-ImageNet and SVHN datasets. The best and second results are highlighted by red and purple colors.

	ResNet-18 on Tiny-ImageNet Adv. Training				ResNet-18 on SVHN Adv. Training			
	Top-1 Err. on Adv. Imgs			Top-1 Err. on Clean Imgs	Top-1 Err. on Adv. Imgs			Top-1 Err. on Clean Imgs
	PGD-10	PGD-30	PGD-50		PGD-10	PGD-30	PGD-50	
ReLU	**67.38%**	84.11%	86.46%	**54.32%**	18.27%	63.71%	71.42%	**6.44%**
ELU	67.98%	85.40%	86.87%	55.06%	18.74%	63.38%	70.72%	6.70%
GELU	67.86%	84.12%	**85.60%**	54.90%	16.76%	61.21%	69.32%	6.98%
FD	70.21%	84.94%	86.35%	57.63%	16.45%	61.85%	69.45%	**6.15%**
DyReLU	67.82%	84.06%	85.90%	55.61%	17.11%	63.50%	70.71%	7.09%
SmReLU	67.95%	85.19%	86.15%	**54.89%**	**16.41%**	**61.00%**	**68.97%**	6.90%
SPARTA	**67.21%**	**83.62%**	**84.70%**	**54.89%**	**15.30%**	**59.29%**	**67.29%**	6.54%

TABLE 8: Comparing the transferred SPARTA with the standard SPARTA and ReLU. The best and second results are highlighted.

Backbone	Activations	Top-1 error on Adv. Images PGD-10	PGD-30	PGD-50	Top-1 err on Clean Img
ResNet-18	ReLU	31.54%	68.93%	75.64%	15.66%
	$\text{SPARTA}_{\text{Res34}}$	**31.06%**	**68.11%**	**75.03%**	15.17%
	$\text{SPARTA}_{\text{Res18}}$	**29.31%**	**65.81%**	**72.55%**	15.48%
ResNet-34	ReLU	31.00%	67.88%	75.15%	17.18%
	$\text{SPARTA}_{\text{Res18}}$	**28.96%**	**65.51%**	**72.40%**	14.60%
	$\text{SPARTA}_{\text{Res34}}$	**29.17%**	**64.13%**	**72.91%**	14.47%

TABLE 9: Transferability of SPARTA across Datasets. The best and second results are highlighted.

Datasets	ResNet-18	Top-1 error on Adv. Images PGD-10	PGD-30	PGD-50	Top-1 err on Clean Img
CIFAR-10	ReLU	31.54%	68.93%	75.64%	15.66%
	$\text{SPARTA}_{\text{SVHN}}$	**30.68%**	**66.93%**	**74.47%**	15.36%
	$\text{SPARTA}_{\text{CIFAR}}$	**29.31%**	**65.81%**	**72.55%**	15.48%
SVHN	ReLU	18.27%	63.71%	71.42%	6.45%
	$\text{SPARTA}_{\text{CIFAR}}$	**16.59%**	**61.88%**	**69.45%**	6.52%
	$\text{SPARTA}_{\text{SVHN}}$	**15.30%**	**59.29%**	**67.29%**	7.05%

18 with SPARTA on CIFAR-10 and obtain the pre-trained SPARTA denoted as $\text{SPARTA}_{\text{CIFAR}}$. Then, we regard $\text{SPARTA}_{\text{CIFAR}}$ as the activation function for another random initialized ResNet-18 and adversarially train it on SVHN to see whether the ResNet-18 with $\text{SPARTA}_{\text{CIFAR}}$ achieves better adversarial robustness or higher accuracy than the one with ReLU and standard SPARTA that are jointly trained with ResNet-18. As shown in Table 9, we observe that: ❶ On both CIFAR-10 and SVHN, ResNet-18 with the transferred SPARTA achieves lower top-1 error rates than the one using ReLU under all three attacks. It demonstrates that *pre-trained* SPARTA *on one dataset still works on another dataset, helping CNN get better adversarial robustness than the vanilla ReLU.* ❷ Compared with the standard case where the parameters of ResNet-18 and SPARTA are jointly updated during adversarial training, ResNet-18 with transferred SPARTA has higher top-1 error rates on adversarial images but lower error rate on clean images.

According to the results in Table 4, we see that: ❶ In general, using SPARTA at deeper groups helps to achieve better adversarial robustness (*i.e.*, lower top-1 error on adversarial examples) as well as better accuracy (*i.e.*, lower top-1 error rate on clean examples). For example, ResNet-18-$G_4.B_2$ achieves the lowest top-1 error on both adversarial and clean examples. ❷ Replacing more ReLU layers is not helpful to obtain even better adversarial robustness or accuracy. For example, ResNet-18-$G_{\{1,2,3,4\}}.B_{\{1,2\}}$ has eight SPARTA layers but obtains higher error rates than $G_{\{1,2,3,4\}}.B_2$ with only four SPARTA layers. Moreover, replacing the last ReLU layers of all groups, *i.e.*, $G_{\{1,2,3,4\}}.B_2$, achieves the best adversarial robustness and the second best accuracy among all variants, indicating the importance of the output activation layers of ResNet groups for adversarial training.

6 CONCLUSIONS

We have proposed a novel activation function, named SPARTA, which is designed to be spatially attentional and adversarially robust. It enables CNNs to achieve higher robustness and accuracy than the ones based on the state-of-the-art activation functions. We have investigated the relationships between SPARTA and the state-of-the-art search-based activation, *i.e.*, Swish, and feature denoising method, providing insights about the advantages of our method. Furthermore, comprehensive evaluation presents two important properties of our method: *superior transferability across CNNs* and *superior transferability across datasets*, confirming SPARTA's important properties of flexibility and versatility.

REFERENCES

[1] C. Szegedy, W. Zaremba, I. Sutskever, J. Bruna, D. Erhan, I. Goodfellow, and R. Fergus, "Intriguing properties of neural networks," *arXiv preprint arXiv:1312.6199*, 2013.

[2] N. Papernot, P. McDaniel, X. Wu, S. Jha, and A. Swami, "Distillation as a defense to adversarial perturbations against deep neural networks," in *2016 IEEE Symposium on Security and Privacy (SP)*. IEEE, 2016, pp. 582–597.

[3] J. Buckman, A. Roy, C. Raffel, and I. Goodfellow, "Thermometer encoding: One hot way to resist adversarial examples," in *International Conference on Learning Representations*, 2018.

[4] C. Xie, J. Wang, Z. Zhang, Z. Ren, and A. Yuille, "Mitigating adversarial effects through randomization," *arXiv preprint arXiv:1711.01991*, 2017.

[5] G. S. Dhillon, K. Azizzadenesheli, Z. C. Lipton, J. Bernstein, J. Kossaifi, A. Khanna, and A. Anandkumar, "Stochastic activation pruning for robust adversarial defense," *arXiv preprint arXiv:1803.01442*, 2018.

[6] X. Liu, M. Cheng, H. Zhang, and C.-J. Hsieh, "Towards robust neural networks via random self-ensemble," in *Proceedings of the European Conference on Computer Vision (ECCV)*, 2018, pp. 369–385.

[7] S. Wang, X. Wang, P. Zhao, W. Wen, D. Kaeli, P. Chin, and X. Lin, "Defensive dropout for hardening deep neural networks under adversarial attacks," in *Proceedings of the International Conference on Computer-Aided Design*, 2018, pp. 1–8.

[8] A. N. Bhagoji, D. Cullina, C. Sitawarin, and P. Mittal, "Enhancing robustness of machine learning systems via data transformations," in *2018 52nd Annual Conference on Information Sciences and Systems (CISS)*. IEEE, 2018, pp. 1–5.

[9] C. Guo, M. Rana, M. Cisse, and L. Van Der Maaten, "Countering adversarial images using input transformations," *arXiv preprint arXiv:1711.00117*, 2017.

[10] A. Prakash, N. Moran, S. Garber, A. DiLillo, and J. Storer, "Deflecting adversarial attacks with pixel deflection," in *Proceedings of the IEEE conference on computer vision and pattern recognition*, 2018, pp. 8571–8580.

[11] Y. Song, T. Kim, S. Nowozin, S. Ermon, and N. Kushman, "Pixeldefend: Leveraging generative models to understand and defend against adversarial examples," *arXiv preprint arXiv:1710.10766*, 2017.

[12] P. Samangouei, M. Kabkab, and R. Chellappa, "Defense-gan: Protecting classifiers against adversarial attacks using generative models," *arXiv preprint arXiv:1805.06605*, 2018.

[13] F. Liao, M. Liang, Y. Dong, T. Pang, X. Hu, and J. Zhu, "Defense against adversarial attacks using high-level representation guided denoiser," in *Proceedings of the IEEE Conference on Computer Vision and Pattern Recognition*, 2018, pp. 1778–1787.

[14] I. J. Goodfellow, J. Shlens, and C. Szegedy, "Explaining and harnessing adversarial examples," *arXiv preprint arXiv:1412.6572*, 2014.

[15] H. Kannan, A. Kurakin, and I. J. Goodfellow, "Adversarial logit pairing," *CoRR*, vol. abs/1803.06373, 2018. [Online]. Available: http://arxiv.org/abs/1803.06373

[16] A. Madry, A. Makelov, L. Schmidt, D. Tsipras, and A. Vladu, "Towards deep learning models resistant to adversarial attacks," *arXiv preprint arXiv:1706.06083*, 2017.

[17] X. Glorot, A. Bordes, and Y. Bengio, "Deep sparse rectifier neural networks," in *Proceedings of the fourteenth international conference on artificial intelligence and statistics*. JMLR Workshop and Conference Proceedings, 2011, pp. 315–323.

[18] A. Krizhevsky, I. Sutskever, and G. E. Hinton, "Imagenet classification with deep convolutional neural networks," *Advances in neural information processing systems*, vol. 25, pp. 1097–1105, 2012.

[19] Y. Chen, X. Dai, M. Liu, D. Chen, L. Yuan, and Z. Liu, "Dynamic relu," in *ECCV*, 2020.

[20] C. Xie, Y. Wu, L. van der Maaten, A. L. Yuille, and K. He, "Feature denoising for improving adversarial robustness," in *IEEE Conference on Computer Vision and Pattern Recognition (CVPR)*, June 2019.

[21] P. Ramachandran, B. Zoph, and Q. V. Le, "Searching for activation functions," *arXiv preprint arXiv:1710.05941*, 2017.

[22] A. Nøkland, "Improving back-propagation by adding an adversarial gradient," *ArXiv*, vol. abs/1510.04189, 2015.

[23] A. Athalye, N. Carlini, and D. Wagner, "Obfuscated gradients give a false sense of security: Circumventing defenses to adversarial examples," in *Proceedings of the 35th International Conference on Machine Learning*, vol. 80, 2018, pp. 274–283.

[24] F. Tramèr, A. Kurakin, N. Papernot, I. J. Goodfellow, D. Boneh, and P. D. McDaniel, "Ensemble adversarial training: Attacks and defenses," in *International Conference on Learning Representations, ICLR 2018*, 2018.

[25] M. Cissé, P. Bojanowski, E. Grave, Y. Dauphin, and N. Usunier, "Parseval networks: Improving robustness to adversarial examples," *ArXiv*, vol. abs/1704.08847, 2017.

[26] M. Hein and M. Andriushchenko, "Formal guarantees on the robustness of a classifier against adversarial manipulation," in *NeurIPS*, 2017.

[27] F. Farnia, J. M. Zhang, and D. Tse, "Generalizable adversarial training via spectral normalization," *ArXiv*, vol. abs/1811.07457, 2019.

[28] G. Li, S. Ding, J. Luo, and C. Liu, "Enhancing intrinsic adversarial robustness via feature pyramid decoder," *IEEE Conference on Computer Vision and Pattern Recognition (CVPR)*, pp. 797–805, 2020.

[29] D. Goodman, X. Li, J. Huan, and T. Wei, "Improving adversarial robustness via attention and adversarial logit pairing," *ArXiv*, vol. abs/1908.11435, 2019.

[30] X. Ma, B. Li, Y. Wang, S. M. Erfani, S. Wijewickrema, G. Schoenebeck, D. Song, M. E. Houle, and J. Bailey, "Characterizing adversarial subspaces using local intrinsic dimensionality," *arXiv preprint arXiv:1801.02613*, 2018.

[31] M. Dong, Y. Li, Y. Wang, and C. Xu, "Adversarially robust neural architectures," *arXiv preprint arXiv:2009.00902*, 2020.

[32] V. Nair and G. E. Hinton, "Rectified linear units improve restricted boltzmann machines." in *ICML*, 2010, pp. 807–814.

[33] A. L. Maas, A. Y. Hannun, and A. Y. Ng, "Rectifier nonlinearities improve neural network acoustic models," in *Proc. icml*, vol. 30, 2013, p. 3.

[34] I. J. Goodfellow, D. Warde-Farley, M. Mirza, A. C. Courville, and Y. Bengio, "Maxout networks." in *ICML (3)*, vol. 28, 2013, pp. 1319–1327.

[35] K. He, X. Zhang, S. Ren, and J. Sun, "Delving deep into rectifiers: Surpassing human-level performance on imagenet classification," in *ICCV*, 2015, pp. 1026–1034.

[36] D.-A. Clevert, T. Unterthiner, and S. Hochreiter, "Fast and accurate deep network learning by exponential linear units (elus)," in *ICLR*, 2016.

[37] J. Hu, L. Shen, and G. Sun, "Squeeze-and-excitation networks," in *2018 IEEE/CVF Conference on Computer Vision and Pattern Recognition*, 2018, pp. 7132–7141.

[38] C. Xie, M. Tan, B. Gong, A. Yuille, and Q. V. Le, "Smooth adversarial training," in *arXiv:2006.14536*, 2020.

[39] D. Hendrycks and K. Gimpel, "Gaussian error linear units (gelus)," *arXiv preprint arXiv:1606.08415*, 2016.

[40] X. Glorot and Y. Bengio, "Understanding the difficulty of training deep feedforward neural networks." in *AISTATS*, vol. 9, 2010, pp. 249–256.

[41] Y. Chen, X. Dai, M. Liu, D. Chen, L. Yuan, and Z. Liu, "Dynamic convolution: Attention over convolution kernels," in *Proceedings of the IEEE/CVF Conference on Computer Vision and Pattern Recognition*, 2020, pp. 11 030–11 039.

[42] K. He, X. Zhang, S. Ren, and J. Sun, "Deep residual learning for image recognition," in *IEEE Conference on Computer Vision and Pattern Recognition (CVPR)*, 2016, pp. 770–778.

[43] A. Madry, A. Makelov, L. Schmidt, D. Tsipras, and A. Vladu, "Towards deep learning models resistant to adversarial attacks." in *ICLR*, 2018.

[44] A. Krizhevsky, G. Hinton *et al.*, "Learning multiple layers of features from tiny images," *University of Toronto, Technical Report*, 2009.

[45] Y. Netzer, T. Wang, A. Coates, A. Bissacco, B. Wu, and A. Y. Ng, "Reading digits in natural images with unsupervised feature learning," in *NIPS Workshop on Deep Learning and Unsupervised Feature Learning 2011*, 2011.